

# STRIPE-LIKE INHOMOGENEITIES, COHERENCE, AND THE PHYSICS OF THE HIGH $T_c$ CUPRATES

J. Ashkenazi

*Physics Department, University of Miami, P.O. Box 248046, Coral Gables, FL 33124, U.S.A.*  
jashkenazi@miami.edu

**Abstract** The carriers in the high- $T_c$  cuprates are found to be polaron-like “stripons” carrying charge and located in stripe-like inhomogeneities, “quasi-electrons” carrying charge and spin, and “svivons” carrying spin and some lattice distortion. The anomalous spectroscopic and transport properties of the cuprates are understood. The stripe-like inhomogeneities result from the Bose condensation of the svivon field, and the speed of their dynamics is determined by the width of the double-svicon neutron-resonance peak. The connection of this peak to the peak-dip-hump gap structure observed below  $T_c$  emerges naturally. Pairing results from transitions between pair states of stripons and quasi-electrons through the exchange of svivons. The pairing symmetry is of the  $d_{x^2-y^2}$  type; however, sign reversal through the charged stripes results in features not characteristic of this symmetry. The phase diagram is determined by pairing and coherence lines within the regime of a Mott transition. Coherence without pairing results in a Fermi-liquid state, and incoherent pairing results in the pseudogap state where localized electron and electron pair states exist within the Hubbard gap. A metal-insulator-transition quantum critical point occurs between these two states at  $T = 0$  when the superconducting state is suppressed. An intrinsic heterogeneity is expected of superconducting and pseudogap nanoscale regions.

**Keywords:** High- $T_c$ , cuprates, stripes, inhomogeneities, pairing symmetry, Mott transition

## 1. Introduction

It is suggested that the anomalous physics of cuprates, including the existence of high- $T_c$  superconductivity, can be understood as the result of a behavior typical of their structure within the regime of a Mott transition. Theoretical calculations, and a variety of experimental data, support the assumption that their microscopic structure, within this regime, is often characterized by dynamic stripe-like inhomogeneities.

To study this regime, a combination of large- $U$  and small- $U$  orbitals is considered, where major aspects within the  $\text{CuO}_2$  planes are approached by the

$t$ - $t'$ - $J$  model. The large- $U$  electrons, residing in these planes, are treated by the “slave-fermion” method [1]. Such an electron in site  $i$  and spin  $\sigma$  is created by  $d_{i\sigma}^\dagger = e_i^\dagger s_{i,-\sigma}$ , if it is in the “upper-Hubbard-band”, and by  $d_{i\sigma}^\dagger = \sigma s_{i\sigma}^\dagger h_i$ , if it is in a Zhang-Rice-type “lower-Hubbard-band”. Here  $e_i$  and  $h_i$  are (“excession” and “holon”) fermion operators, and  $s_{i\sigma}$  are (“spinon”) boson operators. These auxiliary operators have to satisfy the constraint:  $e_i^\dagger e_i + h_i^\dagger h_i + \sum_\sigma s_{i\sigma}^\dagger s_{i\sigma} = 1$ .

An auxiliary space is introduced within which a chemical-potential-like Lagrange multiplier is used to impose the constraint on the average. Physical observables are projected into the physical space by expressing them as combinations of Green’s functions of the auxiliary space. Since the time evolution of Green’s functions is determined by the Hamiltonian which obeys the constraint rigorously, it is not expected to be violated as long as justifiable approximations are used.

The reader is referred to previous publications by the author [2, 3] which include technical details concerning the work discussed here.

## 2. Auxiliary Fields

Uncoupled auxiliary fields are considered at the zeroth order, where the spinon field is diagonalized by applying the Bogoliubov transformation for bosons [4]:

$$s_\sigma(\mathbf{k}) = \cosh(\xi_{\sigma\mathbf{k}})\zeta_\sigma(\mathbf{k}) + \sinh(\xi_{\sigma\mathbf{k}})\zeta_{-\sigma}^\dagger(-\mathbf{k}). \quad (1)$$

Spinon states created by  $\zeta_\sigma^\dagger(\mathbf{k})$  have “bare” energies  $\epsilon^\zeta(\mathbf{k})$ , having a V-shape zero minimum at  $\mathbf{k} = \mathbf{k}_0$ . Bose condensation results in an antiferromagnetic (AF) order of wave vector  $\mathbf{Q} = 2\mathbf{k}_0 = (\frac{\pi}{a}, \frac{\pi}{a})$ . Within the lattice Brillouin zone (BZ) there are four inequivalent possibilities for  $\mathbf{k}_0$ :  $\pm(\frac{\pi}{2a}, \frac{\pi}{2a})$  and  $\pm(\frac{\pi}{2a}, -\frac{\pi}{2a})$ , thus introducing a broken symmetry. One has [4]:

$$\begin{aligned} \cosh(\xi_{\mathbf{k}}) &\rightarrow \begin{cases} +\infty, & \text{for } \mathbf{k} \rightarrow \mathbf{k}_0, \\ 1, & \text{for } \mathbf{k} \text{ far from } \mathbf{k}_0, \end{cases} \\ \sinh(\xi_{\mathbf{k}}) &\rightarrow \begin{cases} -\cosh(\xi_{\mathbf{k}}), & \text{for } \mathbf{k} \rightarrow \mathbf{k}_0, \\ 0, & \text{for } \mathbf{k} \text{ far from } \mathbf{k}_0. \end{cases} \end{aligned} \quad (2)$$

The dynamic stripe-like inhomogeneities are approached adiabatically, treating them statically with respect to the electrons dynamics. Their underlying structure is characterized [5] by narrow charged stripes forming antiphase domain walls between wider AF stripes. Within the one-dimensional charged stripes it is justified to use the spin-charge separation approximation under which two-particle spinon-holon (spinon-excession) Green’s functions are decoupled into single-auxiliary-particle Green’s functions. Holons (excessions)

within the charged stripes are referred to as “stripons” (of charge  $-e$ ), created by  $p_\mu^\dagger(\mathbf{k})$ .

Localized stripon states are assumed at the zeroth order, due to the disordered one-dimensional nature of the charged stripes. Their  $\mathbf{k}$  wave vectors present  $\mathbf{k}$ -symmetrized combinations of localized states to be treated in a perturbation expansion when coupling to the other fields is considered.

Away from the charged stripes, creation operators of approximate fermion basis states of coupled holon-spinon and excision-spinon pairs are constructed [2]. Together with the small- $U$  states they form, within the auxiliary space, a basis to “quasi-electron” (QE) states, created by  $q_{\nu\sigma}^\dagger(\mathbf{k})$ . The bare QE energies  $\epsilon_\nu^q(\mathbf{k})$  form quasi-continuous ranges of bands within the BZ.

When the cuprates are doped, such QE states are transferred from the upper and lower Hubbard bands to the vicinity of the Fermi level ( $E_F$ ). The amount of states transferred is increasing with the doping level, moving from the insulating to the metallic side of the Mott transition regime.

Hopping and hybridization terms introduce strong coupling between the QE, stripon and spinon fields, which is expressed by a coupling Hamiltonian of the form (for p-type cuprates):

$$\begin{aligned} \mathcal{H}' = & \frac{1}{\sqrt{N}} \sum_{\nu\lambda\mu\sigma} \sum_{\mathbf{k},\mathbf{k}'} \{ \sigma \epsilon_{\nu\lambda\mu}^{qp}(\sigma\mathbf{k}, \sigma\mathbf{k}') q_{\nu\sigma}^\dagger(\mathbf{k}) p_\mu(\mathbf{k}') [\cosh(\xi_{\lambda,\sigma}(\mathbf{k}-\mathbf{k}')) \\ & \times \zeta_{\lambda\sigma}(\mathbf{k}-\mathbf{k}') + \sinh(\xi_{\lambda,\sigma}(\mathbf{k}-\mathbf{k}')) \zeta_{\lambda,-\sigma}^\dagger(\mathbf{k}'-\mathbf{k})] + h.c. \}. \end{aligned} \quad (3)$$

Using the formalism of Green’s functions ( $\mathcal{G}$ ), the QE, stripon and spinon propagators are couples by a vertex introduced through  $\mathcal{H}'$  [6].

The stripe-like inhomogeneities are strongly coupled to the lattice, and it is the presence of stripons which creates the charged stripes within them. Consequently, processes involving transitions between stripon and QE states (which, through  $\mathcal{H}'$ , are followed by the emission and/or absorption of spinons) involve also lattice displacements. Since the hopping and hybridization terms depend on the atomic positions [7], the effect of these lattice displacements can be expressed by modifying  $\mathcal{H}'$  in Eq. (3), adding to each of the spinon creation and annihilation operators there a term in which the spinon operator is multiplied by a lattice displacement operator. This introduces a new vertex due to which the spinons are renormalized, becoming “dressed” by phonons, and thus carry some lattice distortion in addition to spin. Such phonon-dressed spinons are referred to as “svivons”, and the physical effect of the new vertex, which is most relevant here, is assumed to be the replacement the spinons by svivons in the  $\mathcal{H}'$  vertex.

The physical signature of the auxiliary fields, within the  $t$ - $t'$ - $J$  model, is demonstrated in Fig. 1, where an adiabatic “snapshot” of a section of a  $\text{CuO}_2$  plane, including a stripe-like inhomogeneity, is shown. Within the adiabatic

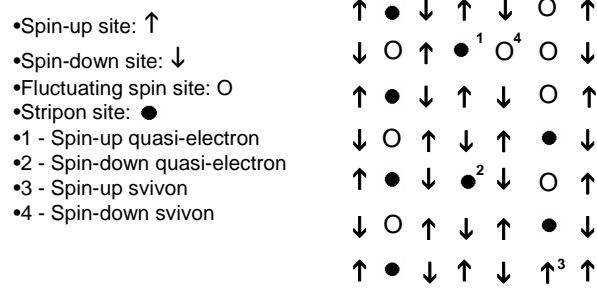


Figure 1. An adiabatic “snapshot” of a stripe-like inhomogeneity and carriers within a  $\text{CuO}_2$  plane.

time scale a site is “spinless” either if it is “charged”, removing the spinned electron/hole on it (as in “stripion sites” in Fig. 1), or if the spin is fluctuating on a shorter time scale (due to, *e.g.*, being in a singlet spin pair). In this description, a site stripion excitation represents a transition between these two types of a spinless site within the charged stripes, a site svivon excitation represents a transition between a spinned site and a fluctuating-spin spinless site, and a site QE excitation represents a transition between a spinned site and a charged spinless site within the AF stripes. The dynamics of these sites is ignored in Fig. 1 for demonstration purposes.

### 3. Auxiliary Spectral Functions

Self-consistent expressions are derived [2] for the spectral functions  $A^q$ ,  $A^p$ , and  $A^\zeta$  for the QE’s, stripions, and svivons, respectively [ $A(\omega) \equiv \Im \mathcal{G}(\omega - i0^+)/\pi$ ], including the scattering rates  $\Gamma^q$ ,  $\Gamma^p$ , and  $\Gamma^\zeta$  [ $\Gamma(\omega) \equiv 2\Im \Sigma(\omega - i0^+)$ ], and the real parts of the self-energies  $\Re \Sigma^q$ ,  $\Re \Sigma^p$  and  $\Re \Sigma^\zeta$ . Since the stripion bandwidth turns out to be considerably smaller than the QE and svivon bandwidths, a phase-space argument could be used, as in the Migdal theorem, to ignore vertex corrections to the  $\mathcal{H}'$  vertex.

The expressions are derived for the intermediary energy range (and the  $T \rightarrow 0$  limit), where the high energy range ( $\gtrsim 0.5$  eV) is treated by introducing cut-off integration limits at  $\pm\omega_c$  (resulting in spurious logarithmic divergencies at  $\pm\omega_c$ ), and the low energy range ( $\lesssim 0.02$  eV) introduces non-analytic behavior at “zero-energy”. The  $\mathbf{k}$  dependence is omitted in the expressions for simplicity, and all the coefficients appearing in them are positive. The expressions for the auxiliary spectral functions are:

$$A^q(\omega) \cong \begin{cases} a_+^q \omega + b_+^q, & \text{for } \omega > 0, \\ -a_-^q \omega + b_-^q, & \text{for } \omega < 0, \end{cases} \quad (4)$$

$$A^p(\omega) \cong \delta(\omega), \quad (5)$$

$$A^\zeta(\omega) \cong \begin{cases} a_+^\zeta \omega + b_+^\zeta, & \text{for } \omega > 0, \\ a_-^\zeta \omega - b_-^\zeta, & \text{for } \omega < 0. \end{cases} \quad (6)$$

Analyticity is restored in the low-energy range, and specifically  $A^\zeta(\omega = 0) = 0$ . Special behavior occurs for svivons around  $\mathbf{k}_0$ . The expressions for the QE and svivon scattering rates are:

$$\frac{\Gamma^q(\omega)}{2\pi} \cong \begin{cases} c_+^q \omega + d_+^q, & \text{for } \omega > 0, \\ -c_-^q \omega + d_-^q, & \text{for } \omega < 0, \end{cases} \quad (7)$$

$$\frac{\Gamma^\zeta(\omega)}{2\pi} \cong \begin{cases} c_+^\zeta \omega + d_+^\zeta, & \text{for } \omega > 0, \\ c_-^\zeta \omega - d_-^\zeta, & \text{for } \omega < 0, \end{cases} \quad (8)$$

and those for the real parts of their self energies are:

$$\begin{aligned} -\Re\Sigma^q(\omega) \cong & \omega_c(c_+^q - c_-^q) + (d_+^q \ln |\frac{\omega - \omega_c}{\omega}| - d_-^q \ln |\frac{\omega + \omega_c}{\omega}|) \\ & + \omega(c_+^q \ln |\frac{\omega - \omega_c}{\omega}| + c_-^q \ln |\frac{\omega + \omega_c}{\omega}|), \end{aligned} \quad (9)$$

$$\begin{aligned} -\Re\Sigma^\zeta(\omega) \cong & \omega_c(c_+^\zeta + c_-^\zeta) + (d_+^\zeta \ln |\frac{\omega - \omega_c}{\omega}| + d_-^\zeta \ln |\frac{\omega + \omega_c}{\omega}|) \\ & + \omega(c_+^\zeta \ln |\frac{\omega - \omega_c}{\omega}| - c_-^\zeta \ln |\frac{\omega + \omega_c}{\omega}|). \end{aligned} \quad (10)$$

The logarithmic divergencies at  $\omega = 0$  are truncated by analyticity in the low-energy range.

For the case of p-type cuprates the following inequalities exist between the coefficients:

$$a_+^q > a_-^q, \quad b_+^q > b_-^q, \quad c_+^q > c_-^q, \quad d_+^q > d_-^q, \quad (11)$$

$$a_+^\zeta > a_-^\zeta, \quad b_+^\zeta > b_-^\zeta, \quad c_+^\zeta > c_-^\zeta, \quad d_+^\zeta > d_-^\zeta. \quad (12)$$

For “real” n-type cuprates, in which the stripons are based on excitation and not holon states, the direction of the inequalities is reversed for the QE coefficients (11), but stays the same for the svivon coefficients (12). Deviations from these inequalities, especially for the  $a_\pm$  and  $b_\pm$  coefficients, could occur due to band-structure effects, and at specific  $\mathbf{k}$  points; by Eq. (2) they almost disappear for svivons close to point  $\mathbf{k}_0$ .

The auxiliary-particle energies are renormalized (from  $\epsilon$  to  $\bar{\epsilon}$ ) through:  $\bar{\epsilon} = \epsilon + \Re\Sigma(\bar{\epsilon})$ . This renormalization is particularly strong for the stripon energies, and their bandwidth drops down to the low energy range [thus having a  $\delta$ -function for  $A^p(\omega)$  in Eq. (5)].

A typical renormalization of the QE energies (for p-type cuprates), around zero energy, is shown in Fig. 2. The kink-like behavior around zero energy is

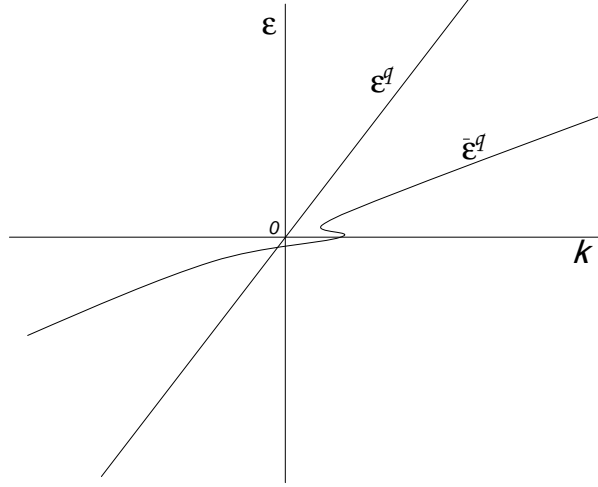


Figure 2. A typical self-energy renormalization of the QE energies, for p-type cuprates.

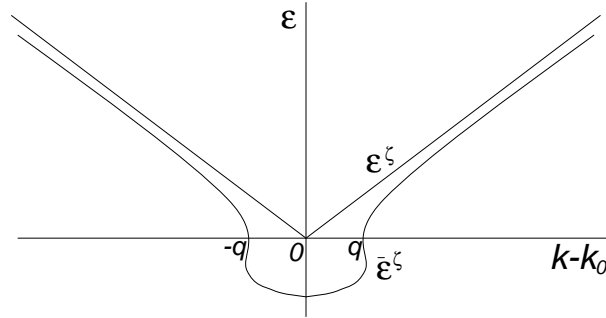


Figure 3. A typical self-energy renormalization of the svivon energies around the minimum at  $\mathbf{k}_0$ .

a consequence of the logarithmic singularity at  $\omega = 0$  (truncated in the low-energy range) in the  $(d_+^q - d_-^q) \ln |\omega|$  term in Eq. (9) for  $\Re \Sigma^q$ . The asymmetry between positive and negative energies is a consequence of inequality (11), and this asymmetry is expected to be inverted for real n-type cuprates.

A typical renormalization of the svivon energies, around the V-shape zero minimum of  $\epsilon^\zeta$  at  $\mathbf{k}_0$ , is shown in Fig. 3. The significant effect results from the  $(d_+^\zeta + d_-^\zeta) \ln |\omega|$  term in Eq. (10) for  $\Re \Sigma^\zeta(\omega)$ , contributing a logarithmic singularity at  $\omega = 0$  (which is truncated in the low-energy range). By Eq. (8)  $\bar{\epsilon}^\zeta$  is expected to have a considerable linewidth around  $\mathbf{k}_0$  (except where it crosses zero). But the existence of a pairing gap in the low-energy QE and

stripon states, coupled by svivons around  $\mathbf{k}_0$ , disables the scattering processes causing the linewidth near the negative minimum of  $\bar{\epsilon}^\zeta$  at  $\mathbf{k}_0$ .

This renormalization of the svivon energies changes the physical signature of their Bose condensation from an AF order to the observed stripe-like inhomogeneities (including both their spin and lattice aspects). The structure of  $\bar{\epsilon}^\zeta$  around its minimum at  $\mathbf{k}_0$  determines the structure of these inhomogeneities, and their dynamics depends on the linewidth of  $\bar{\epsilon}^\zeta$  around  $\mathbf{k}_0$ , becoming slower (and thus detectable) in a pairing state.

As was mentioned above, the stripon states are based on localized states in the charged stripe-like inhomogeneities (see Fig. 1), to which some itineracy is introduced by coupling to the QE and svivon states through  $\mathcal{H}'$ . This implies that their translational symmetry is lower than that of the basic lattice, resulting in a mixture of  $\mathbf{k}$  values of the lattice BZ. Since the charged stripes (where the bare stripon states reside) occupy about a quarter of the  $\text{CuO}_2$  plane, the number of stripon states should be about a quarter of the number of states in this BZ.

The BZ  $\mathbf{k}$  values mostly contributing to the stripon states reflect the structural nature of the stripe-like inhomogeneities, on one hand, and the minimization of free energy due to the  $\mathcal{H}'$ -coupling, on the other hand. Such a minimization is achieved when the stripon  $\mathbf{k}$  values are mainly at BZ areas where the energetic effect of their coupling is the strongest. This would occur for optimal stripon coupling with svivons around  $\mathbf{k}_0$  (see the behavior of  $\bar{\epsilon}^\zeta$  there in Fig. 3), and with QE's at BZ areas of highest density of states (DOS) close to  $E_F$ , which are found in most of the cuprates around the “antinodal” points  $(\frac{\pi}{a}, 0)$  and  $(0, \frac{\pi}{a})$ .

If (from its four possibilities)  $\mathbf{k}_0$  were chosen at  $(\frac{\pi}{2a}, \frac{\pi}{2a})$ , then in order to minimize free energy, the BZ areas (in most of the cuprates) which the  $\mathbf{k}$  values contributing to the stripon states should mostly come from, would be at about a quarter of the BZ around  $\pm\mathbf{k}^p = \pm(\frac{\pi}{2a}, -\frac{\pi}{2a})$  (thus the antinodal points are at  $\mathbf{k}^p \pm \mathbf{k}_0$ ). Stripon states corresponding to an equal mixture of  $\mathbf{k}^p$  and  $-\mathbf{k}^p$  states are created by:

$$\begin{aligned} p_e^\dagger(\pm\mathbf{k}^p) &\propto \sum_i p_i^\dagger \cos \left[ \frac{\pi}{2a}(x_i - y_i) \right], \\ p_o^\dagger(\pm\mathbf{k}^p) &\propto \sum_i p_i^\dagger \sin \left[ \frac{\pi}{2a}(x_i - y_i) \right]. \end{aligned} \quad (13)$$

In the stripe-like inhomogeneity shown in Fig.1 (where the stripes are directed in the  $y$ -direction), one has  $(x_i, y_i) = (4am, an)$ , where  $m$  and  $n$  are integers, and thus  $p_e^\dagger(\pm\mathbf{k}^p)$  creates a state with non-zero amplitudes in the even  $n$  points, while  $p_o^\dagger(\pm\mathbf{k}^p)$  creates a state with non-zero amplitudes in the odd  $n$  points. A similar result would be obtained also in lattice areas where the stripes are

directed in the  $x$ -direction. It will be shown below that pairing occurs between stripon states close to the ones in Eq. (13).

#### 4. Electron Spectrum

Spectroscopic measurements (as in ARPES) based on the transfer of electrons into, or out of, the crystal, are determined by the electron's spectral function  $A_e$ . Projecting the spectral functions from the auxiliary to the physical space [2],  $A_e$  is expressed in terms of QE ( $A^q$ ) and convoluted stripon-svicon ( $A^p A^\zeta$ ) terms. From the quasi-continuum of QE bands, only few, closely related to those of physical electron, contribute “coherent” bands, while the others contribute an “incoherent” background to  $A_e$ .

The electron bands are specified by  $\mathbf{k}$  vectors within the lattice BZ, though the stripe-like inhomogeneities introduce a perturbation of lower periodicity, reflected *e.g.* in “shadow bands”. These bands (as well as the incoherent background in  $A_e$ ) include hybridized contributions of QE states and convoluted stripon–svicon states. As in Eq. (7) for  $\Gamma^q$ , the electronic bandwidths have a  $\propto \omega$  and a constant term, in agreement with experiment.

A significant stripon–svicon contribution to  $A_e$  close to  $E_F$  (at energies around  $\bar{\epsilon}^p \pm \bar{\epsilon}^\zeta$ ) is obtained with svicons around their energy minimum at  $\mathbf{k}_0$  (see Fig. 3). As was discussed above, such a contribution should be found (in most cuprates) in BZ areas around the antinodal points, as has been widely observed (see *e.g.* Ref. [8]).

Such type of a stripon–svicon contribution is not expected close to “nodal” Fermi surface (FS) crossing points, in the vicinity of  $\pm(\frac{\pi}{2a}, \pm\frac{\pi}{2a})$ . Thus the behavior of the electron bands there should be similar to that of the QE bands  $\bar{\epsilon}^q$  (see Fig. 2), having a kink closely below  $E_F$ , as has been observed in ARPES [9, 10]. The observed kink has been attributed to the coupling of electrons to phonons [9] or to the neutron scattering resonance mode [10]. However, such a coupling would generally result in two opposite changes in the band slope (below and above the coupled excitation energy) below  $E_F$ , while the experimental kink looks more consistent with one change in slope below  $E_F$ , as in Fig. 2.

This kink was not found in measurements in the n-type cuprate NCCO [11], which is consistent with the prediction here (suggested by the author earlier [3]) that in real n-type cuprates this kink should be above, and not below  $E_F$  (where ARPES measurements are relevant). Also, there appears to be a sharp upturn in the ARPES band in NCCO [11] very close to  $E_F$  (believed there to be an artifact), which is expected here as the kink is approached from the other side of  $E_F$  (see Fig. 2).

Measurements of the doping-dependence of the slopes of the electron bands around the nodal points [12] show almost no change with doping of the slope



very close to  $E_F$  from below (thus including the kink effect). Here this low-energy slope depends on the nature of the low-energy truncation of the logarithmic singularity in Eq. (9); thus it depends of the width  $\omega^p$  of the stripon band. Our analysis for the thermoelectric power [3], discussed below, predicts  $\omega^p \sim 0.02$  eV, with very weak decrease with doping, which is consistent with the observed slope behavior.

The nodal kink, discussed above, shows almost no change when the temperature is lowered below  $T_c$ , as is expected here. A different type of a kink has been observed around the antinodal points [13, 14], showing a very strong temperature dependence, where its major part appears only below  $T_c$ . Within the present analysis, the temperature dependent part of this antinodal kink originates from the stripon–svivon contribution to the electron bands (discussed above), while the temperature-independent part is of the same origin as the nodal kink (thus due to the QE contribution to the electron bands).

As will be discussed below, the opening of a superconducting (SC) gap causes a decrease in the svivon linewidth around the energy minimum at  $\mathbf{k}_0$ , resulting in the narrowing of the stripon–svivon contribution to the antinodal electron bands below  $T_c$ . This is expressed by the appearance of the temperature-dependent antinodal kink, as well as a peak-dip-hump structure, below  $T_c$  (see discussion below). The appearance of this antinodal kink away from the nodal point on the FS is viewed in ARPES studies, above and below  $T_c$  [15], of FS crossings between the nodal point and half way towards the antinodal point.

The existence of high electron DOS close to  $E_F$  around the antinodal points is actually a consequence of the hybridization between QE’s and convoluted stripon–svivon states of svivons around  $\mathbf{k}_0$ . This has been viewed in ARPES [16] as “an extra low energy scattering mechanism” around the antinodal points. As was discussed above, this could occur when the stripions reside around points  $\pm \mathbf{k}^p$ , which by Eq. (13) is consistent with “vertical stripes” (as those shown in Fig. 1). And indeed, in ARPES measurements in LSCO [17], including both high and low (non-SC) doping levels (which are characterized by “diagonal stripes”), a contribution of  $A_e$  close to  $E_F$  is observed around the nodal points for all doping levels, while around the antinodal points it is observed only for doping levels where the stripes are vertical.

As was demonstrated in Ref. [2],  $t'$  hopping processes (between next-nearest-neighbor sites – along the diagonal) in a  $\text{CuO}_2$  plane, can take place without disrupting the AF order, and thus are only weakly affected by stripes and stripions, while in order for  $t$  hopping processes (between nearest-neighbor sites) to occur without the disruption of the AF order, it is essential for stripions in vertical stripes of  $4a$  separation (as in Fig. 1) to be involved. The existence of nodal electron states close to  $E_F$  is mainly due to  $t'$  processes, while the existence of antinodal electron states close to  $E_F$  is mainly due to  $t$  processes.

## 5. The Neutron Resonance Mode

The imaginary part of the spin susceptibility  $\chi''(\mathbf{q}, \omega)$  (at wave vector  $\mathbf{q}$  and energy  $\omega$ ) has a major contribution from double-svicon excitations which can be expressed [2] as:

$$\begin{aligned} \chi''(\mathbf{q}, \omega) \sim & \sum_{\mathbf{k}} \sinh(2\xi_{\mathbf{k}}) \sinh(2\xi_{\mathbf{q}-\mathbf{k}}) \int d\omega' A^{\zeta}(\mathbf{k}, \omega') \\ & \times \{A^{\zeta}(\mathbf{q}-\mathbf{k}, -\omega-\omega') - A^{\zeta}(\mathbf{q}-\mathbf{k}, \omega-\omega') \\ & + 2A^{\zeta}(\mathbf{q}-\mathbf{k}, \omega'-\omega)[b_T(\omega'-\omega) - b_T(\omega')]\}. \end{aligned} \quad (14)$$

Due to the  $\sinh(2\xi)$  factors, and Eq. (2), large contributions to  $\chi''$  are obtained when both  $\mathbf{k}$  and  $\mathbf{q}-\mathbf{k}$  are close to  $\mathbf{k}_0$ . The effect of the negative minimum of  $\bar{\epsilon}^{\zeta}(\mathbf{k})$  at  $\mathbf{k}_0$ , (see Fig. 3), and specifically in the SC state, where its linewidth is often small, is the existence of a peak in  $\chi''(\mathbf{q}, \omega)$  at  $\mathbf{q} = 2\mathbf{k}_0 = \mathbf{Q}$  (the AF wave vector) and  $\omega = -2\bar{\epsilon}^{\zeta}(\mathbf{k}_0)$ . This peak is consistent with the neutron resonance mode [of energy  $E_{\text{res}} = -2\bar{\epsilon}^{\zeta}(\mathbf{k}_0)$ ], often found in the high- $T_c$  cuprate at  $\sim 0.04$  eV [18, 19]. It is expected here that the energy of this resonance mode has a local maximum, as a function of  $\mathbf{k}$ , at  $\mathbf{k} = \mathbf{Q}$  [since  $\bar{\epsilon}^{\zeta}$  has a minimum at  $\mathbf{k}_0$ ]; however, also a branch of the mode with energy rising with  $\mathbf{k} - \mathbf{Q}$  is expected due to the range where  $\bar{\epsilon}^{\zeta}(\mathbf{k})$  is positive and rising. And indeed, measurements in YBCO [18, 19] show a neutron-scattering peak branch dispersing downward (from the  $\mathbf{k} = \mathbf{Q}$  value), and also one dispersing upward [19]. An approximate circular symmetry around  $\mathbf{k} = \mathbf{Q}$  is obtained [19], as is expected here.

The incommensurate low-energy neutron-scattering peaks, corresponding to the stripe-like inhomogeneities [5], occur at points  $\mathbf{Q} \pm 2\mathbf{q}$ , where the slope of the low-energy  $\bar{\epsilon}^{\zeta}(\mathbf{k})$  is not too steep (see Fig. 3). In the LSCO system the resonance energy at  $\mathbf{k} = \mathbf{Q}$  is higher than the maximal SC gap, and thus a sharp peak is not observed there, being too wide (see discussion below); however, sharp peaks have been observed [20–22] at incommensurate  $\mathbf{Q} \pm 2\mathbf{q}$  points, where the energy is lower than the maximal SC gap. In the LBCO system, the energy dependence of the peak (whether it is sharp or wide) with  $\mathbf{q}$  was also found [23] to have branches dispersing both downward and upward around  $\mathbf{k} = \mathbf{Q}$ . A similar behavior was observed in YBCO<sub>6.6</sub> [24].

Thus, both the resonance mode at  $\mathbf{k} = \mathbf{Q}$ , and the excitations at incommensurate  $\mathbf{Q} \pm 2\mathbf{q}$ , are double-svicon excitations, around its energy minimum at  $\mathbf{k}_0$ , shown in Fig. 3. These are excitations towards the destruction of the stripe-like inhomogeneities; their width determines the speed of the inhomogeneities dynamics, and they exist for stoichiometries where SC exists [21]. Because of the lattice dressing of svivons, these double-svicon excitations are expected to be lattice-dressed spin excitations, and indeed, Cu–O optical phonon modes have been found to be involved in such excitations [25].

Spin excitations in bilayer cuprates are expected [2] to have either odd or even symmetry, with respect to the layers exchange. For odd symmetry one gets results similar to those obtained in the single-layer approach discussed above, while for even symmetry one gets a mode whose energy has a minimum at  $\mathbf{k} = \mathbf{Q}$ , in agreement with experiment [26].

## 6. Transport Properties

Transport properties, unlike *e.g.* ARPES, measure the electrons *within* the crystal, and thus can detect the small energy scale of the stripons, without convoluting them with svivons.

Normal-state transport expressions, *not* including the effect of the pseudogap (PG), were derived [3] using linear response theory, where the zero-energy singularities in the auxiliary spectral functions in Eqs. (4–6) are smoothened in the low-energy range, through Taylor expansion [imposing  $A^\zeta(\omega = 0) = 0$ ]. In this derivation it was taken into account that the electric current can be expressed as a sum  $\mathbf{j} = \mathbf{j}_0^q + \mathbf{j}_0^p$  of contributions of bare QE and stripon states, respectively, and that  $\mathbf{j}_0^p \cong 0$  since the bare stripon states are localized. Thus the contributions to the current of both the QE and the stripon dressed (thus coupled) states originate from  $\mathbf{j}_0^q$ .

Results for the electrical resistivity  $\rho$ , the Hall constant  $R_H$ , the Hall number  $n_H = 1/eR_H$ , the Hall angle  $\theta_H$  (through  $\cot \theta_H = \rho/R_H$ ), and the thermoelectric power (TEP)  $S$ , are presented in Fig. 4. Their anomalous temperature dependencies result both from the low-energy-range stripon band [Eq. (5)], modeled by a “rectangular” shape  $A^p$  of width  $\omega^p$  and fractional occupancy  $n^p$ , and from those of the scattering rates  $\Gamma^q(T, \omega = 0)$  and  $\Gamma^p(T, \omega = 0)$  (see Ref. [3]), including also impurity scattering temperature independent terms.

The transport results in Fig. 4 correspond to five stoichiometries of p-type cuprates, ranging from  $n^p = 0.8$ , corresponding to the underdoped (UD) regime, to  $n^p = 0.4$ , corresponding to the overdoped (OD) regime. The parameter  $N_e^q$  corresponds to the QE contribution to the electrons DOS at  $E_F$ . It is assumed to increase with the doping level  $x$ , reflecting transfer of QE spectral weight from the upper and lower Hubbard bands towards  $E_F$ , while moving from the insulating to the metallic side of the Mott transition regime. Consequently  $\omega^p$  is assumed to decrease somewhat with doping, due to stronger renormalization of the stripon energies [3].

The parameters  $n_H^q$  and  $n_H^p$  represent effective QE and stripon contributions to the density of charge carriers (reflected in the Hall number). Since they both contribute through the current  $\mathbf{j}_0^q$  of the bare QE states, they are expected to have same sign (corresponding to these states). The values of these parameters are assumed to increase with  $x$  (for the same reason that  $N_e^q$  does). Since the coupling between QE’s and stripions grows with  $x$ , and the increase of  $N_e^q$  with

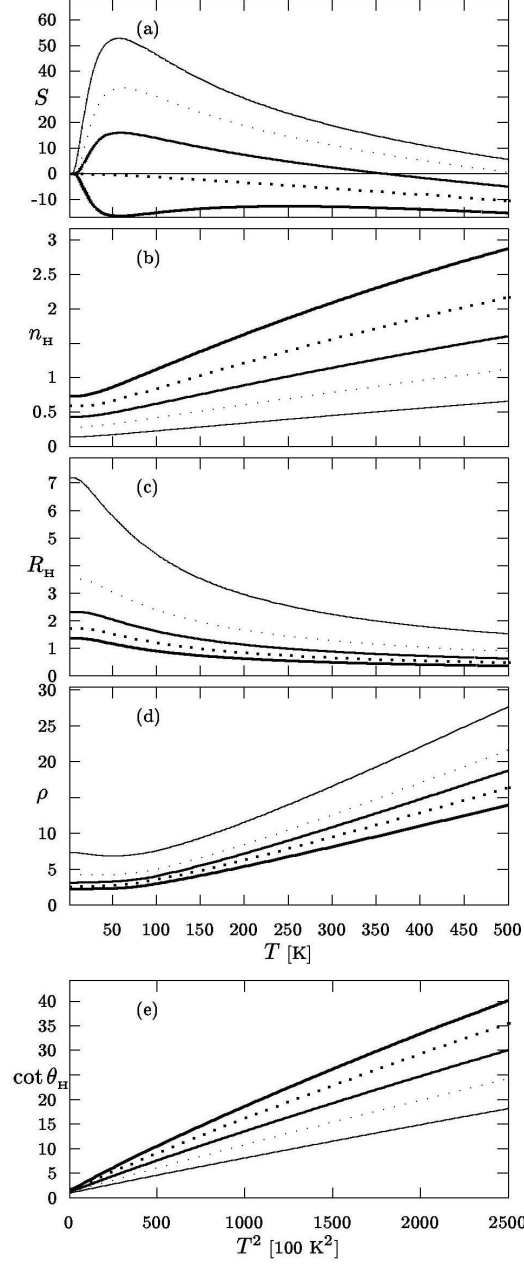


*Figure 4.* The transport coefficients, in arbitrary units [and  $\mu\text{V/K}$  units for  $S$  (a)], for:  $n^p=0.8,0.7,0.6,0.5,0.4$ ;  $10000N_e^q=20,23,26,29,32$ ;  $\omega^p[\text{K}]=200,190,180,170,160$ ;  $n_{\text{H}}^p=0.1,0.2,0.3,0.4,0.5$ ;  $n_{\text{H}}^q=6,7,8,9,10$ ;  $S_1^q=-0.025$ ;  $\gamma_0^p=500$ ;  $\gamma_2^p=0.03$ ;  $\gamma_0^q=5$ ;  $\gamma_1^q=0.2$ . The last values correspond to the thickest lines.

$x$  is slower than that of  $1 - n^p$ , it is assumed that the increase of  $n_H^p$  with  $x$  is faster than that of  $1 - n^p$ , which is faster than that of  $n_H^q$ .

Doping-independent values are assumed for the QE TEP parameter  $S_1^q$  [3] [which is normally negative for p-type cuprates by the inequality (11)], and for the stripon and QE scattering rate parameters  $\gamma_0^p, \gamma_2^p, \gamma_0^q$ , and  $\gamma_1^q$  [3].

The TEP results depend strongly on  $n^p$ , and reproduce very well the doping-dependent experimental behavior [27, 28]. The position of the maximum in  $S$  depends on the choice of  $\omega^p$ , and it may occur below or above  $T_c$  (the existence of a PG may shift it to a higher temperature than predicted here).

Also the results for the Hall coefficients in Fig. 4 reproduce very well the experimental behavior [29, 30]. The anomalous temperature dependence of the  $n_H$  is due to the growing role of  $n_H^q$  in its determination with increasing  $T$ , being dominantly determined by  $n_H^p$  at  $T = 0$ .

The temperature dependence of the resistivity in Fig. 4(d) is linear at high  $T$ , becoming “sublinear” at low  $T$  (for all stoichiometries), while experimentally [31] the low- $T$  behavior crosses over from “superlinearity” in the UD regime, to sublinearity in the OD regime (being linear at low  $T$  for optimally doped cuprates). The superlinear behavior is being generally understood as the effect of the PG (not considered here), and the crossover to sublinear behavior (predicted here) in the OD regime is a natural consequence of the disappearance of the PG with increasing  $x$ .

The TEP in real n-type cuprates is normally expected [3] to behave similarly to the TEP in p-type cuprates, but with an opposite sign and slope. Results for NCCO [32] show such behavior for low doping levels, but in SC doping levels the slope of  $S$  changes from positive to negative, and its behavior resembles that of OD p-type cuprates, shown in Fig. 4(a). This led [3] to the suggestion that NCCO may be not a real n-type cuprate, its stripions being based on holon states (like in p-type cuprates). More recent measurements on the n-type infinite- $\text{CuO}_2$ -layer SLCO [33] do show TEP results for an SC cuprate which have the opposite sign and slope than those of Fig. 4(a) (for p-type cuprates), as is expected for real n-type cuprates (thus with stripions based on excitation states).

As was discussed above, the absence of a kink in the nodal band below  $E_F$  [11] in NCCO, supports the possibility that it is also a real n-type cuprate. It is possible that the change in the sign of the TEP slope in NCCO with doping is an anomalous band-structure effect, probably associated with the peculiar evolution of its FS with doping, detected in ARPES [34]. The position of the kink (below or above  $E_F$ ) is determined by the inequality (11) between  $d_+^q$  and  $d_-^q$ , which is less susceptible to band-structure effects than the inequality (11) between  $b_+^q$  and  $b_-^q$ , determining the sign of the TEP slope. Anomalous behavior is observed also in the Hall constant of NCCO [32], which changes

its sign with temperature in the stoichiometries where the sign of the slope of the TEP has changed.

## 7. Hopping-Induced Pairing

As was demonstrated in Ref. [2], the  $\mathcal{H}'$  vertex enables inter-stripe stripon hopping, through intermediary QE–svivon states. This vertex was also demonstrated [2] to enable inter-stripe hopping of pairs of neighboring stripons through intermediary states of pairs of opposite-spin QE’s, obtained by the exchange of svivons. The pair hopping was shown to result in a gain in inter-stripe hopping energy (compared to the hopping of two uncorrelated stripons), avoiding intermediary svivon excitations. Furthermore, the hybridization of the QE’s with orbitals, beyond the  $t$ – $t'$ – $J$  model, results in further gain in both intra-plane and inter-plane hopping energy.

This provides a pairing scheme based on transitions between pair states of stripons and QE’s through the exchange of svivons. The inter-plane pair hopping, introduced within this scheme, is consistent with  $c$ -axis optical conductivity results [35], revealing (in addition to the opening of the SC gap), the increase of the spectral weight in the mid-IR range (well above the gap) below  $T_c$ . This effect has been observed both in bilayer and single-layer cuprates, and proposed [35] to be the signature of a  $c$ -oriented collective mode emerging (or sharpening) below  $T_c$ . The existence of such a mode below  $T_c$  is due to the hopping of pairs in the  $c$ -direction, during their QE-pair stages, while above  $T_c$ ,  $c$ -axis hopping of stripons (through intermediary QE–svivon states) is, at the most, limited to adjacent  $\text{CuO}_2$  planes.

The pairing diagram (sketched in Ref. [6]) provides Eliasherg-type equations, of coupled stripon and QE pairing order parameters. Coherent pairing occurs [2] between two subsets of the QE and stripon states. For QE’s these subsets are, naturally, of the spin-up ( $\uparrow$ ) and spin-down ( $\downarrow$ ) QE’s. Since the stripons are spinless, their subsets should be determined according to a different criterion.

As was illustrated in Fig. 1, for a  $\text{CuO}_2$  plane within the  $t$ – $t'$ – $J$  model, the  $\uparrow$  QE’s can reside on  $\downarrow$  sites, and the  $\downarrow$  QE’s can reside on  $\uparrow$  sites of the stripe-like inhomogeneities. In Fig. 5 an adiabatic snapshot of an extended section of a stripe-like inhomogeneity is shown, including an expected crossover between stripe segments directed in the  $a$  and the  $b$  directions. Denoted are the *available* sites for the  $\uparrow$  and  $\downarrow$  QE subsets. Since the QE subsets have a spatial interpretation in the  $\text{CuO}_2$  planes (within the adiabatic time scale) it is natural to choose the stripon subsets also on a spatial basis, in a manner which optimizes the coupled pairing.

Since the pairing is optimal between neighboring stripons along the charged stripes [2], the stripon pairing subsets are chosen such that the nearest neigh-

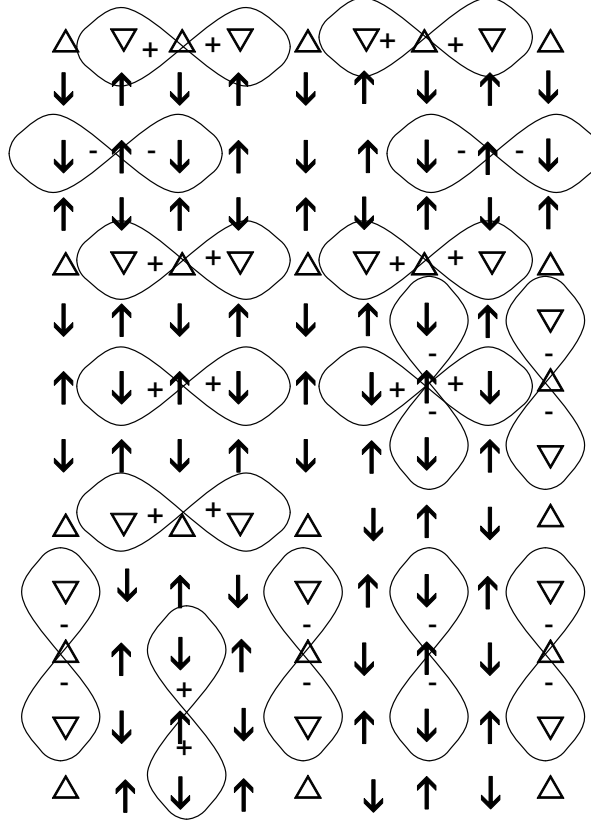


Figure 5. An adiabatic snapshot of an extended section of a stripe-like inhomogeneity, where the available sites for the QE and stripon pairing subsets are illustrated, as well as sketches demonstrating the local symmetry of the pairing order parameters  $\Phi^q$  and  $\Phi^p$ .

bors of a site corresponding to one subset are sites corresponding to the other subset. These subsets are denoted by  $\Delta$  and  $\nabla$ , and the sites *available* for them are shown in Fig. 5 too. Note that each of the stripon states created by  $p_e^\dagger(\pm \mathbf{k}^p)$  and  $p_o^\dagger(\pm \mathbf{k}^p)$ , defined in Eq. (13), belongs to a different subset. This indicates that combinations of stripon states around points  $\pm \mathbf{k}^p$  in the BZ are consistent with this pairing scheme. The required degeneracy of the QE and stripon paired subsets is restored by stripes dynamics.

The QE and stripon pair-correlation functions (pairing order parameters) are defined, within in the position ( $\mathbf{r}$ ) representation, as:

$$\Phi^q(\mathbf{r}_1, \mathbf{r}_2) \equiv \langle q_\uparrow(\mathbf{r}_1) q_\downarrow(\mathbf{r}_2) \rangle, \quad (15)$$

$$\Phi^p(\mathbf{r}_1, \mathbf{r}_2) \equiv \langle p_\Delta(\mathbf{r}_1) p_\nabla(\mathbf{r}_2) \rangle. \quad (16)$$

They are coupled to each other through Eliashberg-type equations, which can be expressed, in the position and the Matsubara ( $\omega_n$ ) representations, as:

$$\begin{aligned} \Phi^q(\mathbf{r}_1, \mathbf{r}_2, i\omega_n) &= \sum_{n'} \int d\mathbf{r}'_1 \int d\mathbf{r}'_2 K^{qp}(\mathbf{r}_1, \mathbf{r}_2, n; \mathbf{r}'_1, \mathbf{r}'_2, n') \\ &\quad \times \Phi^p(\mathbf{r}'_1, \mathbf{r}'_2, i\omega'_n), \end{aligned} \quad (17)$$

$$\begin{aligned} \Phi^p(\mathbf{r}_1, \mathbf{r}_2, i\omega_n) &= \sum_{n'} \int d\mathbf{r}'_1 \int d\mathbf{r}'_2 K^{pq}(\mathbf{r}_1, \mathbf{r}_2, n; \mathbf{r}'_1, \mathbf{r}'_2, n') \\ &\quad \times \Phi^q(\mathbf{r}'_1, \mathbf{r}'_2, i\omega'_n). \end{aligned} \quad (18)$$

Expressions for the kernel functions  $K^{qp}$  and  $K^{pq}$  are obtained from the pairing diagrams; they depend on  $\Phi^q$  and  $\Phi^p$  up to the temperature where the latter vanish. The combination of Eqs. (17) and (18) results in BCS-like equations for both the stripon and the QE order parameters. The coupling between  $\Phi^q$  and  $\Phi^p$  results in maximal pairing between nearest neighbors in the stripe direction, both for stripons and QE's. The resulting local symmetry of  $\Phi^q(\mathbf{r}_1, \mathbf{r}_2)$  and  $\Phi^p(\mathbf{r}_1, \mathbf{r}_2)$  (within the adiabatic time scale) is illustrated in Fig. 5, where point  $\mathbf{r}_1$  is fixed on selected sites (of the  $\uparrow$  and  $\triangle$  QE and stripon subsets), while point  $\mathbf{r}_2$  is varied over the space including the nearest neighbors.

As is illustrated in Fig. 5, the sign of  $\Phi^q$  reverses between the two sides of a charged stripe. This is expected because when two QE sites on different sides of a charged stripe have a stripon site midway between them, then one of them is of  $\uparrow$  and the other is of  $\downarrow$ , and since the exchange of the two fermion operators in the definition of  $\Phi^q$  in Eq. (15) results in sign reversal, there must be sign reversal in  $\Phi^q$  between the two sites. A similar sign reversal has been proposed recently by Fine [36].

The sign of both  $\Phi^q$  and  $\Phi^p$  is expected to be reversed between  $a$ -oriented and  $b$ -oriented stripe segments meeting in a “corner” (shown in Fig. 5). This provides optimal pairing energy, yielding maximal  $|\Phi^q(\mathbf{r}_1, \mathbf{r}_2)|$  when  $\mathbf{r}_1$  and  $\mathbf{r}_2$  are at nearest neighbor QE sites, and zero  $\Phi^q(\mathbf{r}_1, \mathbf{r}_2)$  when  $\mathbf{r}_1$  and  $\mathbf{r}_2$  are at next nearest neighbor sites (where the QE's have the same spin and thus do not pair). Away from the corner regions,  $|\Phi^q(\mathbf{r}_1, \mathbf{r}_2)|$  is maximal when  $\mathbf{r}_1$  and  $\mathbf{r}_2$  are at nearest neighbor QE sites along the stripe direction, but it does not vanish when they are at nearest neighbor sites perpendicular to the stripe direction (which is not implied from Fig. 5).

These symmetry characteristics of  $\Phi^q$  and  $\Phi^p$  are reflected in the symmetry of the physical pairing order parameter. The overall symmetry is expected to be of a  $d_{x^2-y^2}$  type; however, the sign reversal of  $\Phi^q$  through the charged stripes, and the lack of coherence in the details of the dynamic stripe-like inhomogeneities between different  $\text{CuO}_2$  planes, is expected to result in features different from those of a simple  $d_{x^2-y^2}$ -wave pairing (especially when the  $c$ -direction is involved). There is a strong experimental support in the existence



of features of  $d_{x^2-y^2}$ -wave pairing, though different features have been reported too.

## 8. Pairing and Coherence

The pairing mechanism here depends on the stripe-like inhomogeneities, and is expected to be stronger when the AF/stripes effects are stronger, thus closer to the insulating side of the Mott transition regime. Consequently one expects the pairing temperature  $T_{\text{pair}}$  to decrease with the doping level  $x$ , as is sketched in the pairing line in Fig. 6.

The existence of SC requires the existence of not only pairing, but also of phase coherence of the pairing order parameters. Under conditions satisfied for low  $x$  values, within the phase diagram of the cuprates, pairing occurs below  $T_{\text{pair}}$ , while SC occurs only below  $T_{\text{coh}} (< T_{\text{pair}})$ , where phase coherence sets in. The normal-state PG, observed in the cuprates above  $T_c$  (except for high  $x$  values) is a pair-breaking gap at  $T_{\text{coh}} < T < T_{\text{pair}}$  (see Fig. 6). Its size and symmetry are similar to those of the SC gap, and specific heat measurements [37] imply that it accounts for most of the pairing energy. The pairs in the PG state behave similarly to localized bipolarons, and do not contribute to electrical conductivity at low temperatures.

Pairing coherence requires energetic advantage of itineracy of the pairs. Thus  $T_{\text{coh}}$  is expected to increase with  $x$ , as is sketched in the coherence line in Fig. 6, due to moving towards the metallic side of the Mott transition regime. Such a determination of the pairing coherence temperature is consistent with a phenomenological model [38] evaluating  $T_{\text{coh}}$  on the basis of the phase “stiffness”. It yields  $T_{\text{coh}} \propto n_s^*/m_s^*$ , where  $m_s^*$  and  $n_s^*$  are the effective SC pairs mass and density, in agreement with the “Uemura plots” [39] in the PG doping regime.

Similarly, the existence of single-electron coherence in the normal state, namely the existence of a Fermi liquid, depends on the advantage of itineracy of the electronic states near  $E_F$ , resulting in the increase of  $T_{\text{coh}}$  with  $x$  (due to moving towards the metallic side of the Mott transition regime), as is sketched in Fig. 6. Within the non-Fermi-liquid approach used here, the stripe-like inhomogeneities are treated adiabatically. But their dynamics becomes faster above  $T_{\text{pair}}$ , resulting (for  $T_{\text{pair}} < T < T_{\text{coh}}$ ) in a Fermi-liquid state where fast stripe fluctuations may still exist.

ARPES measurements in the OD regime [40] confirm the appearance of coherence effects for  $T_{\text{pair}} < T < T_{\text{coh}}$ . They are found in the nodal and antinodal peaks, and consist of the existence of sharp peak edges and resolved bilayer-split bands. The existence of a coherent three dimensional FS in this regime has been demonstrated through polar angular magnetoresistance oscillations [41].

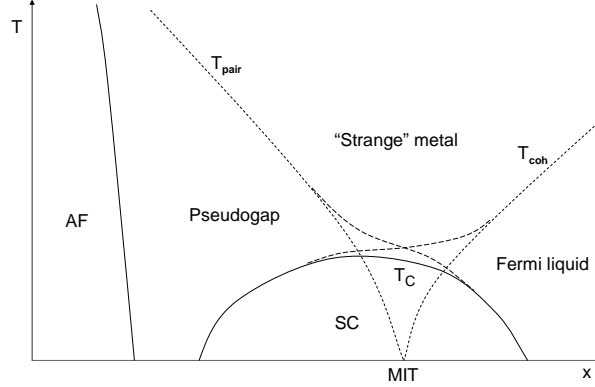


*Figure 6.* A schematic phase diagram for the cuprates. The  $T_c$  line is determined by the pairing line ( $T_{\text{pair}}$ ), decreasing with  $x$ , and the coherence line ( $T_{\text{coh}}$ ), increasing with  $x$ . Broken lines should not be regarded as sharp lines (except when  $T \rightarrow 0$ ), but as crossover regimes. The MIT point is where a metal-insulator transition occurs at  $T = 0$  when SC is suppressed.

Measurements of the in-plane optical conductivity through  $T_c$  [42], show a BCS-type behavior in the OD regime, supporting the existence of Fermi-liquid normal state there (as shown in Fig. 6). On the other hand, in the UD regime these measurements reveal the transfer, below  $T_c$ , of spectral weight from high energies (extending over a broad range up to at least 2 eV), to the infrared range. This behavior has been associated with the establishment of coherence [43]. Within the present approach the PG state consists of localized pairs (and unpaired carriers) within the Hubbard gap, while the establishment of pair coherence in the SC state requires moving states from the upper and lower Hubbard bands into this gap, to contribute to Bloch-like states, explaining the observed transfer of spectral weight.

ARPES measurements on LSCO thin films [44] show that  $T_c$  rises under strain, while the bands close to  $E_F$  become wider. Such a change in the bands is consistent with a move towards the metallic side of the Mott transition regime. Thus we predict that the increase in  $T_c$  under that strain is due to an increase in  $T_{\text{coh}}$ , and that  $T_{\text{pair}}$  (where the PG state sets in) may have decreased in this case.

As is sketched in Fig. 6, there is an increase in the values of  $T_{\text{pair}}$  and  $T_{\text{coh}}$  in the regime where pairing and coherence coexist, compared to their extrapolated values from the regimes where only one of them exists. This is due to the energy gain in the SC state, compared to both the PG and the Fermi-liquid normal states.

If the SC state is suppressed, the occurrence of a metal-insulator transition (MIT) is expected here at  $T = 0$ , at the MIT point in the phase diagram (see Fig. 6), where the metallic phase is of the Fermi-liquid regime, and the in-

ulating phase is of the PG regime of localized electrons and electron pairs within the Hubbard gap. And indeed, experiments where the SC state is suppressed by a magnetic field [45], or by doping [46], show an MIT at  $T \rightarrow 0$ , at  $x \simeq 0.19$ . This stoichiometry corresponds here to a fractional stripon occupancy of  $n^p \simeq \frac{1}{2}$ , as was determined from the TEP results above (see Fig. 4). The existence of the MIT close to this stoichiometry is plausible, because for higher doping levels inter-atomic Coulomb repulsion destabilizes the dynamic charged stripes, essential for the PG state (though the energy gain in the SC state helps maintaining them for higher  $x$ ).

The MIT point in Fig. 6 is a quantum critical point (QCP), and there have been various theoretical approaches addressing the existence of such a QCP. Such approaches often consider different mechanisms for the SC pairing and for the driving force of the PG state, and consequently predict (in difference with the present approach) the existence different regimes of different symmetries, within the SC phase [47]. This has not been confirmed by experiment, in agreement with the present approach. The existence of an intrinsic nanoscale heterogeneity of SC and PG regions [48] will be addressed below.

The connection between SC and an MIT (where the insulating state is due to localization) in the cuprates, as well as in other systems with a similar phase diagram, has been pointed out by Osofsky *et al.* [49]. The conclusion from the present approach is that if a pairing interaction exists, and the insulating state is characterized by the existence of localized pairs at low temperatures, then an SC phase, based on the same pairing interaction, ought to exist around the MIT regime.

## 9. Pairing Gap, Excitations, and the Resonance Mode

The QE and stripon pairing gaps  $2\Delta^q$  and  $2\Delta^p$  are closely related to the order parameters  $\Phi^q$  and  $\Phi^p$  [see Eqs. (15) and (16)], and have the same symmetries. Thus  $\Delta^q$  vanishes at the nodal points and has its maximum  $\Delta_{\text{max}}^q$  at the antinodal points. Since the stripions reside in about a quarter of the BZ around  $\pm \mathbf{k}^p$  [see Eq. (13)],  $|\Delta^p|$  does not vary much from its mean value  $\bar{\Delta}^p$ , and it is greater than the stripon bandwidth  $\omega^p$ , except for the heavily OD regime.

Since the coupled pairing equations (17) and (18) yield in the second order BCS-like equations for both  $\Phi^q$  and  $\Phi^p$ , the QE and stripon single-auxiliary-particle (Bogoliubov) energy bands in a pairing state can be expressed as:

$$E_{\pm}^q(\mathbf{k}) = \pm \sqrt{\bar{\epsilon}^q(\mathbf{k})^2 + \Delta^q(\mathbf{k})^2}, \quad (19)$$

$$E_{\pm}^p(\mathbf{k}) = \pm \sqrt{\bar{\epsilon}^p(\mathbf{k})^2 + \Delta^p(\mathbf{k})^2} \quad (20)$$

(where  $E_{\pm}^p \simeq \pm \Delta^p$  in the UD regime), and the pairing gaps scale with  $T_{\text{pair}}$ , approximately according to the BCS factors, with an increase due to strong-coupling. The relevant factors are of  $s$  pairing for  $\Delta^p$ , and of  $d$  pairing [50] for

$\Delta^q$ :

$$2\bar{\Delta}^p \gtrsim 3.5k_B T_{\text{pair}}, \quad 2\Delta_{\text{max}}^q \gtrsim 4.3k_B T_{\text{pair}}. \quad (21)$$

In the PG state the pairs lack phase coherence, and thus Eq. (19) does not yield a coherence peak in the QE gap edge. Furthermore, in this state the low-energy svivon states are wide, due to incoherence and scattering, and thus the gap is filled with unpaired convoluted stripon–svivon states (see discussion below). Consequently the PG is just a depression of width:

$$2\Delta^{\text{PG}}(\mathbf{k}) = 2\Delta^q(\mathbf{k}) \quad (22)$$

in the DOS, as has been observed, *e.g.* by tunneling spectroscopies [51, 52].

Pairing coherence sets in below  $T_c$ , and the structure of the pair-breaking excitations is determined by the scattering between QE, stripon, and svivon states. This scattering is strong when  $E^q \simeq E^p \pm \bar{\epsilon}^\zeta$ , and particularly for svivon states close to  $\mathbf{k}_0$ , where the  $\cosh(\xi_{\mathbf{k}})$  and  $\sinh(\xi_{\mathbf{k}})$  factors, appearing in the coupling terms, are large [see Eqs. (2) and (3)]. When there are unpaired convoluted stripon–svivon states within the QE gap, paired QE states are scattered to them, resulting in the widening of the QE coherence peak [due to Eq. (19)], at the QE gap edge, to a hump.

The existence of a pairing gap, and especially of the SC gap, limits the scattering of the svivon states around  $\mathbf{k}_0$ , resulting in a decrease in their linewidth. Let  $\mathbf{k}_{\text{min}}$  be the points of small svivon linewidth, for which  $\bar{\epsilon}^\zeta(\mathbf{k}_{\text{min}})$  is the closest to the energy minimum  $\bar{\epsilon}^\zeta(\mathbf{k}_0)$  (see Fig. 3). Often one has  $\mathbf{k}_{\text{min}} = \mathbf{k}_0$ , but there are cases, like that of LSCO, where the linewidth of  $\bar{\epsilon}^\zeta$  is small not at  $\mathbf{k}_0$ , but at close points  $\mathbf{k}_{\text{min}} = \mathbf{k}_0 \pm \mathbf{q}$ . The resonance mode energy  $E_{\text{res}}$  is taken here as  $-2\bar{\epsilon}^\zeta(\mathbf{k}_{\text{min}})$ , accounting both for the generally observed “commensurate mode” at  $Q = 2\mathbf{k}_0$ , and for cases of an “incommensurate mode”, as observed in LSCO at  $\mathbf{Q} \pm 2\mathbf{q}$  [20–22].

The determination of  $\mathbf{k}_{\text{min}}$  is through the limitation of the scattering of a double-svivon excitation of energy  $-2\bar{\epsilon}^\zeta(\mathbf{k}_{\text{min}})$  to a QE pair-breaking excitation of at least the SC gap  $2|\Delta^{\text{SC}}|$ , by exchanging a stripon. If  $2\tilde{\Delta}^{\text{SC}}$  (which is somewhat smaller than the maximal SC gap  $2\Delta_{\text{max}}^{\text{SC}}$ ) is the minimal energy necessary to break a pair of QE’s which are coupled to stripions around  $\pm\mathbf{k}^p$  through a svivon at  $\mathbf{k}_{\text{min}}$ , then this condition can be expressed as:

$$\frac{E_{\text{res}}}{2} = |\bar{\epsilon}^\zeta(\mathbf{k}_{\text{min}})| \leq \tilde{\Delta}^{\text{SC}}. \quad (23)$$

Consequently the svivon energies  $\bar{\epsilon}^\zeta$  have a small linewidth within the range  $|\bar{\epsilon}^\zeta| \leq |\bar{\epsilon}^\zeta(\mathbf{k}_{\text{min}})|$ , and for  $\bar{\epsilon}^\zeta$  within this range, the convoluted stripon–svivon states of energies  $E_+^p \pm |\bar{\epsilon}^\zeta|$  and  $E_-^p \pm |\bar{\epsilon}^\zeta|$  form spectral peaks around

$$\pm E_{\text{peak}}(\mathbf{k}) = E_{\pm}^p(\mathbf{k} \pm \mathbf{k}_0), \quad (24)$$

where to the “basic” peak width:

$$W_{\text{peak}} = 2|\bar{\epsilon}^\zeta(\mathbf{k}_{\min})| = E_{\text{res}} \quad (25)$$

one has to add the effects of the svivon and stripon linewidth, and of the dispersion of  $E_{\pm}^p(\mathbf{k} \pm \mathbf{k}')$  when  $\bar{\epsilon}^\zeta(\mathbf{k}_{\min}) \lesssim \bar{\epsilon}^\zeta(\mathbf{k}') \lesssim 0$  (see Fig. 3). The size of the SC gap is experimentally determined by the spacing between the closest maxima on its two sides. Thus, in the BZ ranges around the antinodal points where  $E_{\text{peak}}(\mathbf{k})$  exists, it often determines the SC gap:

$$|2\Delta^{\text{SC}}(\mathbf{k})| = 2 \min [|\Delta^q(\mathbf{k})|, E_{\text{peak}}(\mathbf{k})]. \quad (26)$$

[Actually, since the peak lies on the slope of the QE gap, its maximum may be shifted to an energy slightly above  $E_{\text{peak}}(\mathbf{k})$ .]  $\Delta^{\text{SC}}$  equals  $\Delta^q$  around its zeroes at the nodal points, which is consistent with the observation by STM [48] that the low energy excitations near the SC gap minimum are not affected by heterogeneity, while the excitations near the gap edge (where it equals  $E_{\text{peak}}$ ) are affected by it (see discussion below). Note that there remain within the SC gap, below the peak, some unpaired convoluted stripon–svivon states corresponding to svivon states of large linewidth and of positive energies  $\bar{\epsilon}^\zeta$  at  $\mathbf{k}$  points farther from  $\mathbf{k}_0$  (see Fig. 3).

As a result, one gets below  $T_c$  a peak-dip-hump structure (on both sides of the gap), where the peak is largely contributed by the convoluted stripon–svivon states around  $E_{\text{peak}}(\mathbf{k})$ , the dip results from the sharp descent at the upper side of this peak, and the hump above them is of the QE gap edge and other states, widened due to scattering to the peak states. Such a structure has been widely observed, *e.g.* by tunneling measurements [51, 52], where the evolution of the gap from a depression in the PG state to a peak-dip-hump structure in the SC state has been viewed. The appearance of the resonance-mode energy  $E_{\text{res}}$  in the peak width in Eq. (25) has been observed in tunneling measurements as the energy separation between the SC gap edge, and the dip for different doping levels [53].

By Eqs. (21), (22), and (26),  $\Delta^{\text{PG}}$  and  $\Delta^{\text{SC}}$  scale with  $T_{\text{pair}}$ , and thus decrease with  $x$ , following the pairing line in Fig. 6, as has been observed. Since  $-\bar{\epsilon}^\zeta(\mathbf{k}_0)$  is zero for an AF, its value (and thus  $E_{\text{res}}$ ) is expected to increase with  $x$ , distancing from an AF state. However, by Eq. (23) its linewidth cannot remain small if it crosses the value of  $\tilde{\Delta}^{\text{SC}}$ , which decreases with  $x$ . Thus the energy  $E_{\text{res}}$  of a *sharp* resonance mode is expected to cross over from an increase to a decrease with  $x$  when it approaches the value of  $2\tilde{\Delta}^{\text{SC}}$ , as has been observed [18]. This crossover could be followed by a shift of the resonance wave vector  $2\mathbf{k}_{\min}$  from the AF wave vector  $\mathbf{Q}$  to incommensurate wave vectors.

Studies of the gap structure by ARPES give information about its  $\mathbf{k}$  dependence, confirming the above features. In bilayer cuprates, the QE bands are

split around the antinodal points into a bonding band (BB) and an antibonding band (AB). On the other hand, the convoluted stripon–svivon peak given by Eqs. (24) and (25) is *not* split and extends over a range of the BZ around the antinodal points. As  $x$  is increased,  $\Delta_{\max}^q$  is decreased, and in the OD regime it is exceeded by  $E_{\text{peak}}(\mathbf{k})$ , at least in a part of the antinodal BZ range [see Eqs. (20) and (24)].

The AB lies very close to  $E_F$ , on the SC gap edge, and consists of Bogoliubov quasiparticles [54] through the antinodal BZ range. In the UD regime the stripon–svivon peak lies within the QE AB gap, reflected in the observation [55] of an AB hump above the peak. On the other hand, in the OD regime the peak lies on the QE AB, or even above it, and consequently the strong scattering which widens the QE band edge coherence peak into a hump is missing. Thus the reported observation is either of one AB peak [13], including the unresolved QE and stripon–svivon contributions, or of two barely resolved peaks [56], where the QE contribution is referred to as an “AB peak”, and the stripon–svivon contribution, lying slightly above it, is referred to as a “BB peak”.

The BB, on the other hand, crosses  $E_F$ , and disperses up to over 0.1 eV from it. Below  $T_c$ , when its distance from  $E_F$  is greater than that of the stripon–svivon peak, it contributes a (QE) hump, referred to [13, 55, 56] as a “BB hump” (though in much of this range its nature is close to that of a normal-state band). In the range where the QE BB overlaps the stripon–svivon peak, the fact that the electron band is formed by their hybridized contributions results in the appearance of the antinodal kink [13–15], due to the narrowing of the peak, as the temperature is lowered below  $T_c$ . This narrowing slows down the stripes dynamics, and widens the “hump states” above the peak. As has been observed [15], this widening (and the resulting band renormalization) has an isotope effect due to the significance of lattice effects in the stripe-like inhomogeneities and in the svivon dressing.

The peak-dip-hump structure has been also observed in tunneling measurements in single-layer BSCO and BSLCO [52], proving that it is not the result of just bilayer splitting. These measurements show that in the PG state above  $T_c$  in BSLCO, the stripon–svivon peak, and the QE hump are merged into one hump. ARPES results in the PG state of BSLCO [57] show an apparent “bilayer splitting” which may indicate that even though the QE and the stripon–svivon contributions to this hump appear merged in tunneling results, they are separated from each other in different  $\mathbf{k}$  points.

In the heavily OD regime, where  $\Delta^{\text{SC}}$  and  $E_{\text{res}}$  become smaller than  $\omega^p$ , the dispersion of  $E_{\text{peak}}(\mathbf{k})$  becomes wider than  $\Delta^{\text{SC}}$  and  $W_{\text{peak}}$  [see Eqs. (20), (24) and (25)]. This results in the smearing of the peak in spectroscopies where it is integrated over the BZ, though it may still be detected in different  $\mathbf{k}$  points [where there remains some smearing, as was mentioned below Eq. (25)]. The apparent disappearance, in the heavily OD regime, of the peak

(of width  $E_{\text{res}}$ ) observed in optical measurements [58] below  $T_c$  may be the result of such smearing (see Ref. [59]). Concerning the question [58] whether the resonance mode is significant for high- $T_c$  SC, the approach presented here considers svivons in the vicinity of  $\mathbf{k}_0$  to be significant for the SC pairing, whether they contribute to the narrow resonance mode peak, or to higher energy excitations [23, 24].

## 10. Heterogeneity and Pairs Density in the SC Phase

The narrow stripon band splits in the SC state, through the Bogoliubov transformation, into the  $E_-^p(\mathbf{k})$  and  $E_+^p(\mathbf{k})$  bands, given in Eq. (20). The states in these bands are created, respectively, by  $p_-^\dagger(\mathbf{k})$  and  $p_+^\dagger(\mathbf{k})$ , which are expressed in terms of creation and annihilation operators of stripions of the two pairing subsets [see Eq. (16)] through equations of the form:

$$\begin{aligned} p_-(\mathbf{k}) &= u_{\mathbf{k}}p_{\Delta}(\mathbf{k}) + v_{\mathbf{k}}p_{\nabla}^\dagger(-\mathbf{k}), \\ p_+^\dagger(\mathbf{k}) &= -v_{\mathbf{k}}p_{\Delta}^\dagger(\mathbf{k}) + u_{\mathbf{k}}p_{\nabla}(-\mathbf{k}), \end{aligned} \quad (27)$$

where  $|u_{\mathbf{k}}|^2 + |v_{\mathbf{k}}|^2 = 1$ .

If all the stripions were paired, then at low temperatures, where the  $E_-^p$  band is completely full, and the  $E_+^p$  band empty, then the fractional stripon occupancy  $n^p$  should have been equal to  $\langle |u_{\mathbf{k}}|^2 \rangle$ . However this cannot be fulfilled in the UD regime, where  $\bar{\Delta}^p$  is considerably greater than the stripon bandwidth  $\omega^p$ , and  $E_{\pm}^p \simeq \pm \Delta^p$ , resulting in  $\langle |u_{\mathbf{k}}|^2 \rangle \simeq \frac{1}{2}$ , while  $n^p > \frac{1}{2}$  (see Fig. 4).

Consequently, in the UD regime, the PG state should consist of *both* paired and unpaired stripions (as was discussed above), and the SC phase should be *intrinsically* heterogenous with nanoscale SC regions, where, locally,  $n^p \simeq \frac{1}{2}$ , and PG regions where, locally  $n^p > \frac{1}{2}$ , such that the correct average  $n^p$  for that stoichiometry is obtained. The size of the regions in this nanostructure should be as small as permitted by the coherence length, and it was indeed observed in nanoscale tunneling measurements in the SC phase [48]. There are, however, physical properties which are determined through a larger scale averaging over these regions. This nanostructure would be naturally pinned to defects, and could become dynamic in very “clean” crystals.

For  $x \simeq 0.19$ , one has  $n^p \simeq \frac{1}{2}$ , and an SC phase could exist without such a nanostructure. Furthermore, in the OD regime  $\bar{\Delta}^p$  becomes comparable, and even smaller than  $\omega^p$ , and the condition  $\langle |u_{\mathbf{k}}|^2 \rangle = n^p$  could be satisfied with all the stripions being paired. Thus the SC phase could exist in the OD regime (especially for  $x \gtrsim 0.19$ ) without the above nanoscale heterogeneity, as has been observed [48].

The Uemura plots [39] give information about the effective density of SC pairs  $n_s^*$ . Within the present approach, the pair states are fluctuating between QE and stripon pair states, and thus  $n_s^*$  is determined by the smaller one, *i.e.*,

the density of stripon pairs. As was discussed above, the stripon band is half full for  $x \simeq 0.19$ , and consequently  $n_s^*$  should be maximal around this stoichiometry, being determined (for p-type cuprates) by the density of hole-like stripon pairs for  $x \lesssim 0.19$ , and of particle-like stripon pairs for  $x \gtrsim 0.19$ . This result is not changed by the intrinsic heterogeneity for  $x \lesssim 0.19$ , since even though the stripon band remains approximately half full within the SC regions, the fraction of space covered by these regions, and thus  $n_s^*$ , is *increasing* with  $x$  in this regime, while in the  $x \gtrsim 0.19$  regime,  $n_s^*$  is *decreasing* with  $x$  because the occupation of stripon band is decreasing below half filling. This result is consistent with the “boomerang-type” behavior [60] of the Uemura plots around  $x \simeq 0.19$ .

Low temperature ARPES results for the spectral weight within the SC peak (omitting the background including the hump), integrated over the antinodal BZ area [61], reveal a maximum for  $x \simeq 0.19$  (similarly to  $n_s^*$ ). This is expected here, assuming that the integrated spectral weight counted is dominantly within the stripon–svivon peak (discussed above), and that this peak counts the major part of SC hole-like pair-breaking excitations of stripsons within the  $E_-^p$  band, as is expected. For the intrinsically heterogenous  $x \lesssim 0.19$  regime, the integrated weight within the peak is expected to increase with  $x$  because of the increase in the fraction of space covered by the SC regions (keeping the stripon band approximately half full within these region). For the  $x \gtrsim 0.19$  regime the integrated weight, measured by ARPES, scales with  $\langle |u_{\mathbf{k}}|^2 \rangle$ , and is thus decreasing with  $x$  below half filling of the stripon band. Note that the contribution of the QE AB to the ARPES peak had to be omitted [61] in order to get the decrease of the peak weight for  $x \gtrsim 0.19$ , confirming that this behavior is due to the stripon–svivon peak, as is suggested here.

## 11. Conclusions

The anomalous properties of the cuprates, including the occurrence of high- $T_c$  superconductivity, are found to be a result typical of their electronic and lattice structure, within the regime of a Mott transition. On one hand, hopping-induced pairing, which depends on dynamical stripe-like inhomogeneities, is stronger for low doping levels, closer to the insulating side of the Mott transition regime. On the other hand, phase coherence, which is necessary for superconductivity to occur, is stronger for high doping levels, closer to the metallic side of the Mott transition regime. Pairing without coherence results in the pseudogap state of localized electrons and electron pairs, and coherence without pairing results in a Fermi-liquid normal state. Suppression of superconductivity results in a quantum critical point of a metal-insulator transition between these two states at  $T = 0$ . An intrinsic heterogeneity exists of nanoscale superconducting and pseudogap regions.



## References

- [1] S. E. Barnes, *Adv. Phys.* **30**, 801 (1980).
- [2] J. Ashkenazi, *J. Phys. Chem. Solids*, **65**, 1461 (2004); cond-mat/0308153.
- [3] J. Ashkenazi, *J. Phys. Chem. Solids*, **63**, 2277 (2002); cond-mat/0108383.
- [4] J. Ashkenazi, *J. Supercond.* **7**, 719 (1994).
- [5] J. M. Tranquada *et al.*, *Phys. Rev. B* **54**, 7489 (1996); *Phys. Rev. Lett.* **78**, 338 (1997).
- [6] J. Ashkenazi, *High-Temperature Superconductivity*, edited by S. E. Barnes, J. Ashkenazi, J. L. Cohn, and F. Zuo (AIP Conference Proceedings 483, 1999), p. 12; cond-mat/9905172.
- [7] E. Pavarini, *et al.*, *Phys. Rev. Lett.* **87**, 047003 (2001).
- [8] T. Yoshida, *et al.*, *Phys. Rev. B* **63**, 220501 (2001).
- [9] A. Lanzara, *et al.*, *Nature* **412**, 510 (2001).
- [10] P. D. Johnson, *et al.*, *Phys. Rev. Lett.* **87**, 177007 (2001).
- [11] N. P. Armitage, *et al.*, *Phys. Rev. B* **68**, 064517 (2003).
- [12] X. J. Zhou, *et al.*, *Nature* **423**, 398 (2003).
- [13] A. D. Gromko, *et al.*, *Phys. Rev. B* **68**, 174520 (2003).
- [14] T. Sato, *et al.*, *Phys. Rev. Lett.* **91**, 157003 (2003).
- [15] G.-H. Gweon, *et al.*, *Nature* **430**, 187 (2004); A. Lanzara, *et al.*, these proceedings.
- [16] X. J. Zhou, *et al.*, *Phys. Rev. Lett.* **92**, 187001 (2004).
- [17] T. Yoshida, *et al.*, *Phys. Rev. Lett.* **91**, 027001 (2003).
- [18] Ph. Bourges, *et al.*, *Science* **288**, 1234 (2000); cond-mat/0211227; Y. Sidis, *et al.*, cond-mat/0401328.
- [19] D. Reznik, *et al.*, cond-mat/0307591.
- [20] J. M. Tranquada, *et al.*, *Phys. Rev. B* **69**, 174507 (2004).
- [21] S. Wakimoto, *et al.*, *Phys. Rev. Lett.* **92**, 217004 (2004).
- [22] N. B. Christensen, *et al.*, cond-mat/0403439.
- [23] J. M. Tranquada, *et al.*, *Nature* **429**, 534 (2004).
- [24] S. M. Hayden, *et al.*, *Nature* **429**, 531 (2004).
- [25] R. J. McQueeney, *et al.*, *Phys. Rev. Lett.* **87**, 077001 (2001); J.-H. Cunniff, *et al.*, *Phys. Rev. B* **67**, 014517 (2003); L. Pintschovius, *et al.*, cond-mat/0308357; T. Cuk, *et al.*, cond-mat/0403521; T. Egami, these proceedings, views the lattice effect as the primary one; M. V. Eremin and I. Eremin, these proceedings, consider spin-lattice coupling.
- [26] Ph. Bourges, *et al.*, *Phys. Rev. B* **56**, R12439 (1997); S. Pailhes, *et al.*, *Phys. Rev. Lett.* **91**, 23700 (2003); cond-mat/0403609.
- [27] B. Fisher, *et al.*, *J. Supercond.* **1**, 53 (1988); J. Genossar, *et al.*, *Physica C* **157**, 320 (1989).
- [28] S. Tanaka, *et al.*, *J. Phys. Soc. Japan* **61**, 1271 (1992); K. Matsuura, *et al.*, *Phys. Rev. B* **46**, 11923 (1992); S. D. Obertelli, *et al.*, *ibid.*, p. 14928; C. K. Subramaniam, *et al.*, *Physica C* **203**, 298 (1992).
- [29] Y. Kubo and T. Manako, *Physica C* **197**, 378 (1992).
- [30] H. Y. Hwang, *et al.*, *ibid.* **72**, 2636 (1994).
- [31] H. Takagi, *et al.*, *Phys. Rev. Lett.* **69**, 2975 (1992).

- [32] J. Takeda, *et al.*, *Physica C* **231**, 293 (1994); X.-Q. Xu, *et al.*, *Phys. Rev. B* **45**, 7356 (1992); Wu Jiang, *et al.*, *Phys. Rev. Lett.* **73**, 1291 (1994).
- [33] G. V. M. Williams, *et al.*, *Phys. Rev. B* **65**, 224520 (2002).
- [34] N. P. Armitage, *et al.*, *Phys. Rev. Lett.* **88**, 257001 (2002).
- [35] M. Gruninger, *et al.*, *Phys. Rev. Lett.* **84**, 1575 (2000); D. N. Basov, *Phys. Rev. B* **63**, 134514 (2001); A. B. Kuzmenko, *et al.*, *Phys. Rev. Lett.* **91**, 037004 (2003).
- [36] B. V. Fine, cond-mat/0308428; these proceedings.
- [37] I. Tifrea, and C. P. Moca, *Eur. Phys. J. B* **35**, 33 (2003).
- [38] V. J. Emery, and S. A. Kivelson, *Nature* **374**, 4347 (1995); *Phys. Rev. Lett.* **74**, 3253 (1995); cond-mat/9710059.
- [39] Y. J. Uemura, *et al.*, *Phys. Rev. Lett.* **62**, 2317 (1989).
- [40] Z. M. Yusof, *et al.*, *Phys. Rev. Lett.* **88**, 167006 (2002); A. Kaminski, *et al.*, *Phys. Rev. Lett.* **90**, 207003 (2003).
- [41] N. E. Hussey, *et al.*, *Nature* **425**, 814 (2004).
- [42] H. J. A. Molegraaf, *et al.*, *Science* **295**, 2239 (2002); A. F. Santander-Syro, *et al.*, *Europhys. Lett.* **62**, 568 (2003); cond-mat/0405264; C. C. Homes, *et al.*, *Phys. Rev. B* **69**, 024514 (2004).
- [43] M. R. Norman, and C. Pepin, *Phys. Rev. B* **66**, 100506 (2002); cond-mat/0302347.
- [44] M. Abrecht, *et al.*, *Phys. Rev. Lett.* **91**, 057002 (2003); D. Pavuna, *et al.*, these proceedings.
- [45] G. S. Boebinger, *et al.*, *Phys. Rev. Lett.* **77**, 5417 (1996).
- [46] J. L. Tallon, and J. W. Loram, *Physica C* **349**, 53 (2001); C. Panagopoulos, *et al.*, *Phys. Rev. B* **69**, 144510 (2004); S. H. Naqib, *et al.*, cond-mat/0312443.
- [47] E.g.: David Pines, these proceedings; C. M. Varma, these proceedings.
- [48] K. McElroy, *et al.*, *Nature* **422**, 592 (2003); cond-mat/0404005.
- [49] M. S. Osofsky, *et al.*, *Phys. Rev. B* **66**, 020502 (2002); these proceedings.
- [50] H. Won, and K. Maki, *Phys. Rev. B* **49**, 1397 (1994).
- [51] Ch. Renner, *et al.*, *Phys. Rev. Lett.* **80**, 149 (1998); M. Suzuki, and T. Watanabe, *Phys. Rev. Lett.* **85**, 4787 (2000).
- [52] M. Kugler, *et al.*, *Phys. Rev. Lett.* **86**, 4911 (2001); A. Yurgens, *et al.*, *Phys. Rev. Lett.* **90**, 147005 (2003).
- [53] J. F. Zasadzinski, *et al.*, *Phys. Rev. Lett.* **87**, 067005 (2001); M. Oda, *et al.*, these proceedings.
- [54] H. Matsui, *et al.*, *Phys. Rev. Lett.* **90**, 217002 (2003).
- [55] S. V. Borisenko, *et al.*, *Phys. Rev. Lett.* **90**, 207001 (2003); T. K. Kim, *et al.*, *Phys. Rev. Lett.* **91**, 177002 (2003).
- [56] D. L. Feng, *et al.*, *Phys. Rev. Lett.* **86**, 5550 (2001).
- [57] C. Janowitz, *et al.*, *Europhys. Lett.* **60**, 615 (2002); cond-mat/0107089.
- [58] J. Hwang, *et al.*, *Nature* **427**, 714 (2004).
- [59] T. Cuk, *et al.*, cond-mat/0403743.
- [60] Ch. Niedermayer, *et al.*, *Phys. Rev. Lett.* **71**, 1764 (1993).
- [61] D. L. Feng, *et al.*, *Science* **289**, 277 (2000); H. Ding, *et al.*, *Phys. Rev. Lett.* **87**, 227001 (2001); R. H. He, *et al.*, *Phys. Rev. B* **69**, 220502 (2004).